Supporting information.

Experimental.

Materials. Tin(II) phthalocyanine ($Sn^{II}Pc$, TCI), tin(VI) phthalocyanine dichloride ($Sn^{VI}Cl_2Pc$, TCI), tin(VI) naphthalocyanine dichloride ($Sn^{VI}Cl_2Nc$, >95%, TCI), tetrabutylammonium bromide (TBABr, >99%, Aldrich), tetrabutylammonium chloride (TBACl, >99%, Aldrich), 4,7,13,16,21,24-hexaoxa-1,10-diazabicyclo[8.8.8]hexacosane (Cryptand[2.2.2], >99%, TCI), bis(pentamethylcyclopentadienyl) cobalt(II) (Cp^*_2Co, Sigma-Aldrich), bis(pentamethylcyclopentadienyl) chromium(II) (Cp^*_2Cr, >95%, Strem), (pentamethylcyclopentadienyl) iridium(III) dichloride dimer ($\{Cp^*IrCl_2\}_2$, >95%, TCI), diiodo(pentamethylcyclopentadienyl)iridium(III) dimer ($\{Cp^*IrI_2\}_2$, Sigma-Aldrich), dichloro(pentamethylcyclopentadienyl)iridium(III) dimer ($\{Cp^*IrCl_2\}_2$, >95%, TCI), cyclopentadienylvanadium tetracarbonyl ($CpV(CO)_4$, >97%, Aldrich), cyclopentadienylmolybdenium tricarbonyl dimer ($\{CpMo(CO)_3]_2$, >98%, Strem), chloro(1,5-cyclooctadiene)iridium(I) dimer ($\{(COD)IrCl\}_2$, >99%, Strem), dichloro(benzene)ruthenium(II) dimer ($\{(C_6H_6)RuCl_2\}_2$, >98%, Strem), triirondodecacarbonyl ($Fe_3(CO)_{12}$, contains 1-10% of methanol, Sigma-Aldrich), osmium carbonyl ($Os_3(CO)_{12}$, >99%, Strem), iridium carbonyl ($Ir_4(CO)_{12}$, >98%, Strem), violanthrone (98%, TCI), and potassium graphite (KC_8, Strem) were used as received. Sodium fluorenone ketyl was obtained according to Ref. [1]. Solvents were purified in an argon atmosphere and degassed. *o*-Dichlorobenzene ($C_6H_4Cl_2$) was distilled over CaH_2 under reduced pressure, benzonitrile was distilled over Na under reduced pressure, and *n*-hexane was distilled over Na/benzophenone. All manipulations for the syntheses of **1-13** were carried out in an MBraun 150B-G glove box with a controlled argon atmosphere and the content of H_2O and O_2 less than 1 ppm. The solvents and crystals were stored in a glove box. Polycrystalline samples of **6**, **10-12** were placed in quartz tubes of 2 mm diameter under argon and sealed at ambient pressure for SQUID and EPR measurements.

KBr pellets for IR- and UV-visible-NIR measurements for **2-13** were prepared in a glove box.

General. UV-visible-NIR spectra of **2-13** were measured in KBr pellets on a Perkin Elmer Lambda 1050 spectrometer in the 250-2500 nm range. FT-IR spectra of **2-13** were obtained in KBr pellets with a Perkin-Elmer Spectrum 400 spectrometer (400-7800 cm^{-1}). A Quantum Design MPMS-XL SQUID magnetometer was used to measure static magnetic susceptibility of **6**, **10**-**12** at 100 mT magnetic field in cooling and heating conditions in the 300 − 1.9 K range. A sample holder contribution and core temperature-independent diamagnetic susceptibility (χ_d) were subtracted from the experimental values. The χ_d values were estimated by the extrapolation of the data in the high-temperature range by fitting the data with the expression: $\chi_M = C/(T - \Theta) + \chi_d$, where C is Curie constant and Θ is Weiss temperature. Effective magnetic moment (μ_{eff}) was calculated with the following formula: $\mu_{eff} = (8\chi_M T)^{1/2}$.

Synthesis. The crystals of **1-13** were obtained by diffusion technique. A reaction mixture was cooled down to room temperature and filtered into a glass tube for diffusion of 1.8 cm diameter and 50 mL volume with a ground glass plug, and then 30 mL of *n*-hexane was layered over the solution. Slow mixing of two solutions resulted in precipitation of the crystals over 1-2 months. The solvent was then decanted from the crystals, and they were washed with several portions of *n*-hexane. The compositions of the obtained complexes were determined from X-ray diffraction analysis on a single crystal. Several crystals from each synthesis tested by X-ray diffraction were found to consist of one single crystalline phase. The determined composition was confirmed by elemental analysis for relatively stable complexes **2-5**. Due to high air sensitivity of **6-13** elemental analysis could not be used to confirm the composition because they reacted with oxygen in the air before the quantitative oxidation procedure could be performed. That is explained by the presence of air-sensitive $Pc^{\bullet 3-}$ radical trianions and metal fragments.

Previously $\{Cp^*Ir^{III}I_2 \cdot Sn^{II}(Pc^{2-})\} \cdot 2C_6H_4Cl_2$ was obtained and structurally characterized by reduction of fullerene C_{70} and $Sn^{II}Pc$ with sodium fluorenone ketyl in the presence of TBABr with the following interaction of the obtained reaction mixture with the $\{Cp^*Ir^{III}I_2\}_2$ dimer.[2] We carried out a similar reaction with the $\{Cp^*Ir^{III}Cl_2\}_2$ dimer and violanthrone dye trying to obtain a three-component complex based on them. In this case a small amount of good quality crystals of solvent free phase $[Cp^*Ir^{III}Cl_2 \cdot Sn^{II}(Pc^{2-})]$ (**1**) was obtained. The reduction of tin(II) phthalocyanine (26.6 mg, 0.042 mmol) and violanthrone (19.1 mg, 0.042 mmol) in 17 ml of $C_6H_4Cl_2$ with sodium fluorenone ketyl (22 mg, 0.108 mmol) in the presence of two equivalents of TBABr (26.8 mg, 0.084 mmol) during one day at 60°C yielded deep blue solution. This solution was filtered into a flask containing the $(Cp^*Ir^{III}Cl_2)_2$ dimer (16.8 mg, 0.022 mmol). The solution was mixed additionally for 24 hours to form a green solution. Slow mixing with *n*-hexane produced a small amount of black blocks of good quality but in low yield (only several single crystals were obtained). Since these crystals had unit cell parameters differing from those of previously studied $\{Cp^*Ir^{III}I_2 \cdot Sn^{II}(Pc^{2-})\} \cdot 2C_6H_4Cl_2$,[1] we investigated crystal structure of **1**. That was the new solvent free phase $[Cp^*Ir^{III}Cl_2 \cdot Sn^{II}(Pc^{2-})]$ (**1**). Here we present only its crystal structure.

For the preparation of the crystals of $[Cp^*Ir^{III}I_2 \cdot Sn^{II}(Pc^{2-})] \cdot C_6H_4Cl_2$ (**2**), tin(II) phthalocyanine (26.6 mg, 0.042 mmol) and half equivalent of the $(Cp^*Ir^{III}I_2)_2$ dimer (24.3 mg, 0.021 mmol) were stirred during 24 hours at 50°C. Phthalocyanine dissolved to form a green solution. Slow mixing with *n*-hexane produced black blocks of good quality which were isolated, washed with *n*-hexane and dried (62% yield). Previously crystals of another phase $\{Cp^*Ir^{III}I_2 \cdot Sn^{II}(Pc^{2-})\} \cdot 2C_6H_4Cl_2$were obtained in other experimental conditions.[2] Since obtained crystals of **2** had different unit cell parameters, we investigated the crystal structure of **2**. That was a phase with a lower content of *o*-dichlorobenzene molecules. Crystals were obtained in a 38% yield as black plates. Composition determined from X-ray diffraction on a single crystal

was confirmed by elemental analysis: $C_{48}H_{35}Cl_2I_2IrN_8Sn$, M_r = 1359.43. Calculated: C, 42.41; H, 2.57; N, 8.24; Found: C, 42.21; H, 2.34; N, 7.98.

The crystals of $[CpV(CO)_3{\cdot}Sn^{II}(Pc^{2-})]{\cdot}C_6H_4Cl_2$ (**3**) were obtained by the interaction of tin(II) phthalocyanine (26.6 mg, 0.042 mmol) and two equivalents of $CpV(CO)_4$ (19 mg, 0.084 mmol) in 17 ml of $C_6H_4Cl_2$ during one day at 50°C. Phthalocyanine dissolved to form deep green solution. Crystals of **3** were obtained as black plates in a 52% yield. The composition of **3** determined from X-ray diffraction on a single crystal was confirmed by elemental analysis: $C_{46}H_{25}Cl_2N_8O_3SnV$, M_r = 978.27. Calculated: C, 56.47; H, 2.55; N, 11.45, Cl 7.26; Found: C, 56.11; H, 2.31; N, 11.22; Cl 7.04.

Since previously obtained complex $[(Cp^*Mo^{II}(CO)_2Br{\cdot}Sn^{II}(Pc^{2-})]{\cdot}0.5C_6H_4Cl_2$ (**16**) contained a non-integer amount of Br (approximately 0.83 per formula unit),[3] we tried to substitute bromide anions at Mo^{II} atoms by chloride anions. The crystals of $[CpMo^{II}(CO)_2Cl{\cdot}Sn^{II}(Pc^{2-})]{\cdot}C_6H_4Cl_2$ (**4**) were obtained by the following procedure. Fullerene C_{60} (30 mg, 0.042 mmol) was reduced by a slight excess of sodium fluorenone ketyl (11 mg, 0.054 mmol) in the presence of one equivalent of TBACl (13.4 mg, 0.042 mmol). After one day fullerene salt was obtained, and the solution was filtered into a flask containing 30 mg of $Sn^{IV}Cl_2Pc$ (0.042 mmol). Phthalocyanine dissolved to form deep blue solution, and after one day one equivalent of the cyclopentadienylmolybdenium tricarbonyl dimer, $\{CpMo(CO)_3]_2$, was added (20.4 mg, 0.084 mmol). The color of the solution changed to deep green within half an hour. This color preserved after one day of stirring. Crystals of **4** were obtained as black plates in a 48% yield. The composition of **4** determined from X-ray diffraction on a single crystal was confirmed by elemental analysis: $C_{45}H_{25}Cl_3O_2MoN_8Sn$, 1030.71. Calculated: C, 52.43; H, 2.43; N, 10.87, Cl 10.33; Found: C, 52.15; H, 2.21; N, 10.43; Cl 10.02.

The crystals of $[\{CpMo(CO)_2\}{\cdot}\{Sn^{II}(Pc^{2-})\}_2]{\cdot}4C_6H_4Cl_2$ (**5**) were obtained by the following procedure. Tin(II) phthalocyanine (26.6 mg, 0.042 mmol) and half equivalent

of the cyclopentadienylmolybdenium tricarbonyl dimer, $\{CpMo(CO)_3]_2$ (10.2 mg, 0.021 mmol), were mixed during one day at 50°C. Phthalocyanine dissolved to form greenish-blue solution. Crystals of **5** were obtained as black rods in a 16% yield. Composition of **5** determined from X-ray diffraction on a single crystal was confirmed by elemental analysis: $C_{95}H_{53}O_2MoN_{16}Sn_2Cl_8$, Mr = 2067.45: C, 55.19; H, 2.56; N, 10.83, Cl 13.74. Found: C, 54.78; H, 2.28; N, 10.42; Cl 14.12.

Crystals of $\{Cryptand(Na^+))[(COD)IrCl{\cdot}Sn^{II}(Pc^{\bullet 3-})]^-{\cdot}2C_6H_4Cl_2$ (**6**) were prepared by using $\{Cryptand(Na^+)\}[Sn^{II}(Pc^{\bullet 3-})]^-$ salt which was obtained in solution by reduction of tin(II) phthalocyanine (26.6 mg, 0.042 mmol) with 11 mg of sodium fluorenone ketyl (0.056 mmol) in the presence of one equivalent of cryptand (16 mg, 0.042 mmol). Deep blue solution was formed. It was filtered into a flask containing the $\{(COD)IrCl\}_2$ dimer (14.1 mg, 0.042 mmol). Deep blue color of the solution was preserved and after one month crystals of **6** were obtained in a 44% yield. Crystals were obtained as black plates, respectively, with a size up to 0.5×0.5×0.3 mm^3. $C_{70}H_{72}Cl_5IrN_{10}NaO_6Sn$, M_r = 1660.50. Calculated: C, 50.63; H, 4.36; N, 8.43; Cl 10.69; Found: C, 49.87; H, 4.05; N, 8.12; Cl 10.54.

Crystals of $\{Cp^*_2Co^+)[Cp^*IrI_2{\cdot}Sn^{II}(Pc^{\bullet 3-})]^-{\cdot}2C_6H_4Cl_2$ (**7**) were prepared by the following procedure: tin(II) phthalocyanine (26.6 mg, 0.042 mmol) and 24.3 mg of the $(Cp^*Ir^{III}I_2)_2$ dimer (0.021 mmol) were stirred at 50°C during 24 hours. A deep green solution formed. It was filtered into a flask containing Cp^*_2Co (13.5 mg, 0.042 mmol). The color of the solution changed to deep blue. After one month the crystals of **8** were obtained as black prisms in a 64% yield. Crystals for IR and UV-visible-NIR spectra were tested by X-ray diffraction.

$(TBA^+)[Fe(CO)_4{\cdot}Sn^{II}(Pc^{\bullet 3-})]^-$ (**8**) were prepared by reduction of tin(II) phthalocyanine (26.6 mg, 0.042 mmol) by 11 mg of sodium fluorenone ketyl (0.056 mmol) in the presence of one equivalent of TBABr (13.5 mg, 0.042 mmol) by stirring *o*-

dichlorobenzene solution (17 mL) during 24 hours at 50°C. Deep blue solution was filtered into a flask containing 21 mg $Fe_3(CO)_{12}$ (0.042 mmol). Deep blue color was preserved. The crystals of **8** were formed after one month as black plates in a 72% yield. Crystals for IR and UV-visible-NIR spectra were tested by X-ray diffraction.

Previously crystals of $\{Cryptand(Na^+)\}[Fe(CO)_4[Sn^{II}(Pc^{\bullet 3-})]^-\cdot 1/3C_6H_4Cl_2$ (**22**) were obtained and studied.[3] They were formed when sodium fluorenone ketyl was used as a reductant. Crystals of $\{Cryptand(K^+))[Fe(CO)_4\cdot Sn^{II}(Pc^{\bullet 3-})]\cdot 2C_6H_4Cl_2$ (**9**) were prepared by another method. Tin(II) phthalocyanine (26.6 mg, 0.042 mmol) was reduced by an excess of potassium graphite (20 mg, 0.145 mmol) in the presence of one equivalent of cryptand (16 mg, 0.042 mmol) by stirring the *o*-dichlorobenzene solution (17 mL) during 24 hours at 50°C. Deep blue solution of $\{Cryptand(Na^+)\}\{Sn^{II}(Pc^{\bullet 3-})\}^-$ formed. It was filtered into a flask containing 21 mg of $Fe_3(CO)_{12}$ (0.042 mmol). Deep blue color of the solution was preserved. After one month black plates with characteristic copper luster were obtained on the walls of the tube in a 53% yield. These crystals had unit cell parameters different from those of previously studied $\{Cryptand(Na^+)\}[Fe(CO)_4[Sn^{II}(Pc^{\bullet 3-})]^-\cdot 1/3C_6H_4Cl_2$ (**23**),[3] and correspondingly $\{Cryptand(K^+))[Fe(CO)_4\cdot Sn^{II}(Pc^{\bullet 3-})]\cdot 2C_6H_4Cl_2$ (**9**) had different crystal structure and composition. Therefore, even small changes in size of the counter cations can affect crystal structure and packing of these complexes. The compound was obtained as dark black blocks in a 43% yield. Crystals for IR and UV-visible-NIR spectra were tested by X-ray diffraction.

Crystals of $\{Cryptand(Na^+)\}[(C_6H_6)RuCl\cdot\{Sn^{II}(Pc^{\bullet 3-})\}_2]\cdot 2.75C_6H_4Cl_2$ (**10**) were prepared by using $\{Cryptand(Na^+)\}[Sn^{II}(Pc^{\bullet 3-})]^-$ salt which was generated in *o*-dichlorobenzene (17 mL) by reduction of tin(II) phthalocyanine (26.6 mg, 0.042 mmol) with 11 mg of sodium fluorenone ketyl (0.056 mmol) in the presence of one equivalent of cryptand (16 mg, 0.042 mmol) by stirring during 24 hours at 50°C . Deep blue solution is

formed. It was filtered into a flask containing 10.6 mg of the $\{(C_6H_6)RuCl_2\}_2$ dimer (0.021 mmol). Deep blue color of the solution was preserved and after one month the crystals of **10** were obtained as black plates in a 48% yield. $C_{101.5}H_{83}Cl_{5.5}N_{18}NaO_6RuSn_2$, M_r = 2207.27. Calculated: C, 55.23; H, 3.76; N, 11.42; Cl 8.84; Found: C, 54.79; H, 3.48; N, 11.22; Cl 8.71.

Crystals of $\{Cp^*_2Cr^+)[Ir_4(CO)_{11}\cdot Sn^{II}(Pc^{\bullet 3-})]^-\cdot C_6H_4Cl_2$ (**11**) were prepared by reduction of half equivalent of $Sn^{VI}Cl_2Pc$ (15 mg, 0.021 mmol) by one equivalent of Cp^*_2Cr (13.5 mg, 0.042 mmol) in *o*-dichlorobenzene (17 mL) by stirring during 24 hours at 50°C. Deep blue solution formed. Half equivalent of iridium carbonyl (23.1 mg, 0.021 mmol) was added. Deep blue color of the solution was preserved, and the crystals of **11** were obtained after one month as black bulks in a 51% yield. $C_{69}H_{50}Cl_2CrIr_4N_8O_{11}Sn$, M_r = 2177.56. Calculated: C, 38.06; H, 2.30; N, 5.14; Cl 3.26; Found: C, 37.58; H, 2.04; N, 5.02; Cl 3.14.

Crystals of $\{Cp^*_2Cr^+)[Ir_4(CO)_{11})\cdot Sn^{II}(Nc^{\bullet 3-})]^-\cdot C_6H_4Cl_2$ (**12**) were prepared by reduction of half equivalent of $Sn^{VI}Cl_2Nc$ (18.9 mg, 0.021 mmol) by one equivalent of Cp^*_2Cr (13.5 mg, 0.042 mmol) in *o*-dichlorobenzene (17 mL) by stirring during 24 hours at 50°C. Naphthalocyanine dissolved to form deep blue-green solution. Half equivalent of iridium carbonyl (23.1 mg, 0.021 mmol) was added, deep blue-green color was preserved and the crystals of **12** were obtained as black needles after one month in a 38% yield. $C_{91}H_{62}Cl_4CrIr_4N_8O_{11}Sn$, M_r = 2524.77. Calculated: C, 43.29; H, 2.46; N, 4.44; Cl 5.62; Found: C, 42.81; H, 2.19; N, 4.22; Cl 5.41.

Crystals of $\{Cp^*_2Cr^+)[Os_3(CO)_{11}\cdot Sn^{II}(Nc^{\bullet 3-})]^-2C_6H_4Cl_2$ (**13**) were prepared by reduction of half equivalent of $Sn^{VI}Cl_2Nc$ (18.9 mg, 0.021 mmol) by Cp^*_2Cr (13.5 mg, 0.042 mmol) in *o*-dichlorobenzene (17 mL) by stirring during 24 hours at 50°C. As a result, deep blue-green solution formed. Half equivalent of osmium carbonyl (19.0 mg, 0.021 mmol) was added preserving deep blue-green color of the solution, and the crystals

of **13** were obtained as black blocks after one month in a 49% yield. Crystals for IR and UV-visible-NIR spectra were tested by X-ray diffraction.

References.

1 D. V. Konarev, S. S. Khasanov, E. I. Yudanova and R. N. Lyubovskaya, *Eur. J. Inorg. Chem.* 2011, 816–820.

2 D. V. Konarev, S. I. Troyanov, A. V. Kuzmin, Y. Nakano, S. S. Khasanov, A. Otsuka, H. Yamochi, G. Saito and R. N. Lyubovskaya, *Organometallics*, 2015, **34**, 879–89.

3 D. V. Konarev, A. V. Kuzmin, Y. Nakano, M. A. Faraonov, S. S. Khasanov, A. Otsuka, H. Yamochi, G. Saito and R. N. Lyubovskaya, *Inorg. Chem*., 2016, **55**, 1390–1402.

IR-spectra

Table S1. IR spectra of starting compounds and complexes **2** – **5.**

Comp.	$Sn^{II}(Pc^{2-})$	$\{Cp^*IrI_2\}_2$	$[Cp^*IrI_2 \cdot Sn^{II}(Pc^{2-})] \cdot C_6H_4Cl_2$ (**2**)	$CpV(CO)_4$	$[CpV(CO)_3 \cdot Sn^{II}(Pc^{2-})] \cdot C_6H_4Cl_2$ (**3**)	$\{CpMo(CO)_3\}_2$	$[CpMo^{II}(CO)_2Cl \cdot Sn^{II}(Pc^{2-})]_2 \cdot C_6H_4Cl_2$ (**4**)	$[CpMo(CO)_2 \cdot Sn^{II}(Pc^{2-})]_2 \cdot 4C_6H_4Cl_2$ (**5**)
Tin phthalo-cyanine	435w 498w 627w 725m 745m 768m 819w 872w 887m 948w 1059s 1072s 1114s 1156w 1283m 1329s 1407w 1454w 1486s 3049w	-	436w 504w 630w 727s 750m* 777w 825w - 892m - - 1077m 1117m* - 1287w 1334s - 1455w* 1497w -	-	- 507w* - 724m 751w* 775w 826w* 874w 892w 956w - 1078m 1121m* 1163w 1290w 1334m 1418w 1459w* 1478w	-	435w 502w* - 727s 750m* 773w 811w - 891m - - 1075m 1119s* 1164w 1289w 1333s - 1456w* 1491w -	- 499w* 629w 726m 748w* 763w 818m* - 891m - - 1079s 1117s* 1165w 1289w 1331m - 1463w* - -
Transition metal fragment	-	Cp^*IrI_2 423w 534w 607w 951w 1021s 1076w 1153w 1356s 1370m 1381s 1417w 1459s 1618w 2901w 2960w 2979w	Cp^*IrI_2 - - - - - 1377w - - 1418w - - - - - -	$CpV(CO)_4$ 432w 498m 596m 625w 837m 1013w CO 1895s 2015m	$CpV(CO)_4$ - 507w* - - 826w* - CO 1824s 1832s 1861w 1974m 1985s 2019s 2036s 2075s	417w 451m 477w 501m 547m 587m 824s 1016w 1264w 1419w 1427w CO 1886s 1899s 1953s 3115w	$CpMo(CO)_2$ - - 480w 502w* 543w - 823w - - 1418w - - 1862s 1956s - -	$CpMo(CO)_2$ - - - 499w* 553m - 818m* - 1261w 1417w - - 1867m 1930w - -
Solvent	-	-	$C_6H_4Cl_2$ 658w 750m* 1033w 1117m* 1455w*	-	$C_6H_4Cl_2$ - 751w* - 1121m* 1459w*	-	$C_6H_4Cl_2$ 658w 750m* 1036w 1119s0 1456w**	$C_6H_4Cl_2$ - 748w* - 1117s* 1463w*

* - bands are coincided; w – weak, m –middle and s – strong intensity

Table S2. IR spectra of starting compounds and complexes **6** and **7**

Comp.	$Sn^{II}(Pc^{\bullet 3-})$ in {cryptand(Na^+)} $[Sn^{II}(Pc^{\bullet 3-})]^-$ $\cdot C_6H_4Cl_2$	Cryptand	{IrCl (COD)}$_2$	{Cryptand(Na^+)} $[(COD)Ir^{I}Cl\cdot Sn^{II}(Pc^{\bullet 3-})]^-\cdot 2C_6H_4Cl_2$ (**6**)	M-fragment	{$Cp^*_2Co^+$}{$[Cp^*IrI_2][Sn^{II}(Pc^{\bullet 3-})]$}$\cdot 2C_6H_4Cl_2$ (**7**)
Tin Phthalo-cyanine	499w 716s 740m 766m 817w 927w 1003w 1051m 1103s 1112s 1163w 1288w 1298w 1325w 1356w 1417w 1457m 2865w 2914w 2967w 3050w	-	-	496w* 714m 748m* 766w 822w 928w* 1006w* 1048m 1102s* 1113s* 1165w* - 1299m* 1327m* 1354w* 1420w 1456m* 2869w - - -		- 711m* 748w* 765w 824w - - 1044m* 1086m* 1113m* 1163w* 1288w - 1328w* - 1420m* 1455w* - 2927w 2972w* -
$Cation^+$	-	476w 735m 922m 948w 982m 1038w 1071m 1100s 1127s 1295m 1329m 1360s 1446m 1462m 1490w 2877w 2943w		Cryptand(Na^+) 468w - 928w* 950w - 1038w* 1088s* 1102s* 1113s* 1299m* 1327m* 1354w* 1433w - 1498w 2879w* -	$Cp^*_2Co^+$ 445w 717w 1024s 1078m 1260w 1314m 1376s 1425m 1452m 1474m 1612s 2850w 2904w 2960w	$Cp^*_2Co^+$ 442s 711m* - 1086m* 1264w 1328w* - 1420m* 1455w* 1563w* - - 2899w* 2972w*
Transitio n metal fragment	-	-	412s 496s 507m 530s 783w 806w 831m 900s 967m 978m 999m 1073w 1154w 1321w 2877w	IrCl(COD) - 496w* - - - - - - - - 1006w* 1088s* 1165w* 2879w*	Cp^*IrI_2 423w 534w 951w 1021s 1076w 1153w 1356s 1370m 1381s 1417w 1459s 1618w 2901w 2960w 2979w	Cp^*IrI_2 - - - - 1086m* 1163w* - 1378w - 1420m* 1563w* 1630w 2899w* - 2972w*
Solvent	-	-	-	$C_6H_4Cl_2$ 748m* 1038w* 1113s* 1456m*		$C_6H_4Cl_2$ 748w* 1044m* 1113m* 1563w*

* - bands are coincided; w – weak, m –middle and s – strong intensity

Table S3. IR spectra of starting compounds and complexes **8-10**

Comp.	$Sn^{II}(Pc^{\bullet 3-})$ in {cryptand(Na^+)} $[Sn^{II}(Pc^{\bullet 3-})]^{\bullet -}$ $\cdot C_6H_4Cl_2$	TBA^+	$Fe_3(CO)_{12}$	(TBA^+) {$[Fe(CO)_4 \cdot Sn^{II}(Pc^{\bullet 3-})]$} (**8**)	{Crypt(Na^+)) $[Fe(CO)_4 \cdot Sn^{II}(Pc^{\bullet 3-})]\} \cdot 2C_6H_4Cl_2$ (**9**)	(C_6H_6) $RuCl_2$	{Cryptand(Na^+)} $[(C_6H_6)RuCl_2 \cdot \{Sn^{II}(Pc^{\bullet 3-})\}_2] \cdot C_6H_4Cl_2$ (**10**)
Tin Phthalo-cyanine	499w 628w 657w 716s 740m 766m 817w 894w 927w 941w 1003w 1051m 1103s 1112s 1163w 1288w 1298w 1325w 1356w 1417w 1457m 1601w 2817w 2865w 2914w 2967w 3050w	-	-	502w 627m - 710w 747w* 764w 829w 890w* - 947w 1001w* - - 1116m* 1166w* 1288w - 1330m - 1416w 1460w* 1603w - 2874w* 2930w 2961w* 3053w	498w 626m - 712w 748w* 768w 820w 892w 927w* 940w* 1004w 1054w 1101m* 1116s* 1166w - 1300w* 1330w* 1354w* 1421w 1464w* 1602w 2821w 2866w* 2906w 2961w 3051w		498w 631w 657w* 713s 746m* 764w 822w 884w 928w* 942w* 1001w* 1053w* 1102s* 1115s* 1165w - 1300m* 1327m* 1356w* 1419m 1456m* 1601w 2816w 2866w* - 2967w 3054w
TBA^+	-	TBA^+ 738s 883s 896s 922s 992s 1031m 1059m 1069m 1110s 1166s 1240m 1365m 1379m 1455s 1464s 1474s 2873w 2959w	-	TBA^+ 747w* - 890w* 1001w* - - - 1080w 1116m* 1166w* - - 1380w - 1460w* - 2874w* 2961w*	Cryptand(Na^+) - - 731w 927w* 940w* 1037w* 1089m 1101m* 1116s* - 1300w* 1330w* 1354w* 1436w 1464w* 1501w 2866w*		Cryptand(Na^+) 466w - 746m* 928w* 942w* 1034w* 1088s 1102s* 1115s* - 1300m* 1327m* 1356w* - 1456m* 1498w 2866w*
Transition metal fragment	-	-	415w 573s 596s 1044w CO 1830s 1859m 2024s 2104m	- 568w - - CO 1896s 1928w 2015m -	- 568w - 1037w* CO 1908s 1933s 2014s -	444m 618w 841s 900w 954w 974m 1015w 1149w 1431s 3033w 3076w	438w - - - 942w* - 1001w* - 1434m - -

* - bands are coincided; w – weak, m –middle and s – strong intensity

Table S4. IR spectra of starting compounds and complex **11-13.**

Components	$Sn^{II}(Pc^{\bullet 3-})$	$Cp^{*}{}_2Cr$	$Ir_4(CO)_{12}$	$\{Cp^*{}_2Cr^+)\{[Ir_4(CO)_{11}\cdot Sn^{II}(Pc^{\bullet 3-})]\cdot C_6H_4Cl_2$ (**11**)	$Sn^{II}(Nc^{2-})$	$\{Cp^*{}_2Cr^+)[Ir_4(CO)_{11}\cdot Sn^{II}(Nc^{\bullet 3-})]\cdot C_6H_4Cl_2$(**12**)	$Os_3(CO)_{12}$	$\{Cp^*{}_2Cr^+)[Os_3(CO)_{11}\cdot Sn^{II}(Nc^{\bullet 3-})]\cdot 2C_6H_4Cl_2$ (**13**)
Tin phthalocyanine	499w 657w 716s 740m 766m 817w 894w 927w 941w 1003w 1051m 1103s 1112s 1163w 1288w 1298w 1325w 1356w 1417w 1457m 1601w 2865w 2914w 2967w 3050w	-	-	- 659w* 714s 748m* 766m 827w 886w - 949w 999w - - 1114s* 1166m - 1306w 1328m - 1421m* 1456m 1603w - 2921w - 3056w	467m 486w 565w 615w 709m 717w 727w 748m 808w 884w 1013m 1025m 1079s 1122w 1147w 1261w 1318w 1336w 1359m 1469w 1504w 1624w 2859w 2926w 2957w	472w* - - - - 714w - 756w* - 889w - - 1090m - - 1261w* 1323w 1341m 1356m - - - - - - -		464w - 565w* - 712w - - 750w* 800w* 884w - 1020w* 1091m - 1159w 1263w* - 1340m 1355m - - - - - - -
$Cation^+$	-	$Cp^{*}{}_2Cr^+$ 587w 800w 1019m 1067w 1262w 1375m 1417w 1446w 2955w	-	$Cp^*{}_2Cr^+$ - 799w* 1022w* 1084m 1252s* 1384m 1421m* 1434w -		$Cp^*{}_2Cr^+$ - - - - 1261w* - - - -		$Cp^*{}_2Cr^+$ 586m* 800w* 1020w* - 1263w* - - 1455w* -
Transition metal fragment	-	-	440m 471w 498s 529m 805w 1022w 1104w 1260w CO 2024s 2059s 2087s	$Ir_4(CO)_{12}$ 438w 474w - 525m 799w* 1022w* - 1252s* CO 1816s 1839s 1996s 2007s 2035s 2045s 2074s		$Ir_4(CO)_{12}$ - 1472w* - 525w - - - 1261w* CO 1817m 2001s 2043s 2078w	$Os_3(CO)_{12}$ 410w 431w 463w 496w 563w 584m 604m CO 1984s 1994s 2016s 2028s 2040s 2060s 2068s	$Os_3(CO)_{12}$ 412w - - 496w 565w* 586m* 605m CO 1986s 1994s 2016s 2039s 2068s - -
$C_6H_4Cl_2$	-	-	-	659w* 748m* 1036w 1114s* 1462w		- 756w* - - -		

* - bands are coincided; w – weak, m –middle and s – strong intensity

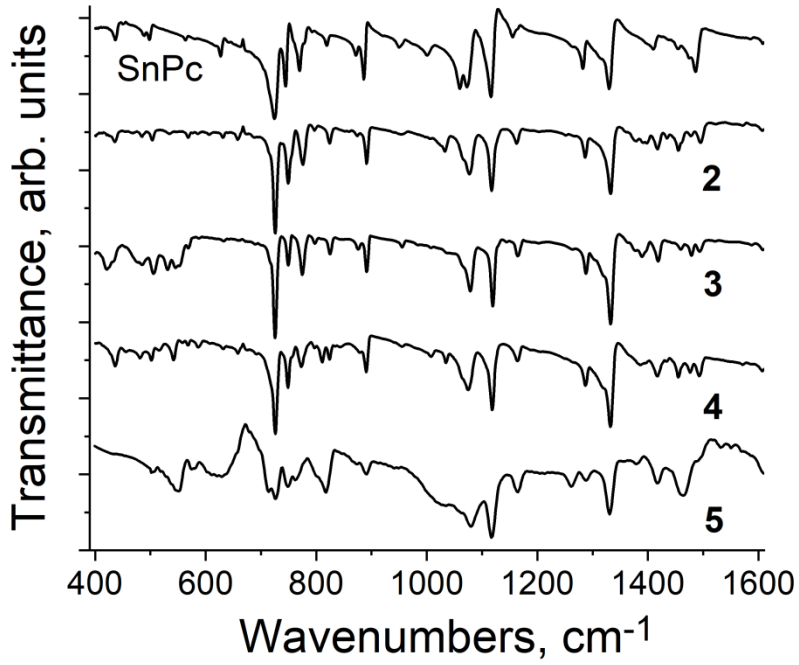

Figure S1. IR spectra of pristine neutral $Sn^{II}Pc$ and compounds **1** - **5** in KBr pellets prepared in anaerobic conditions

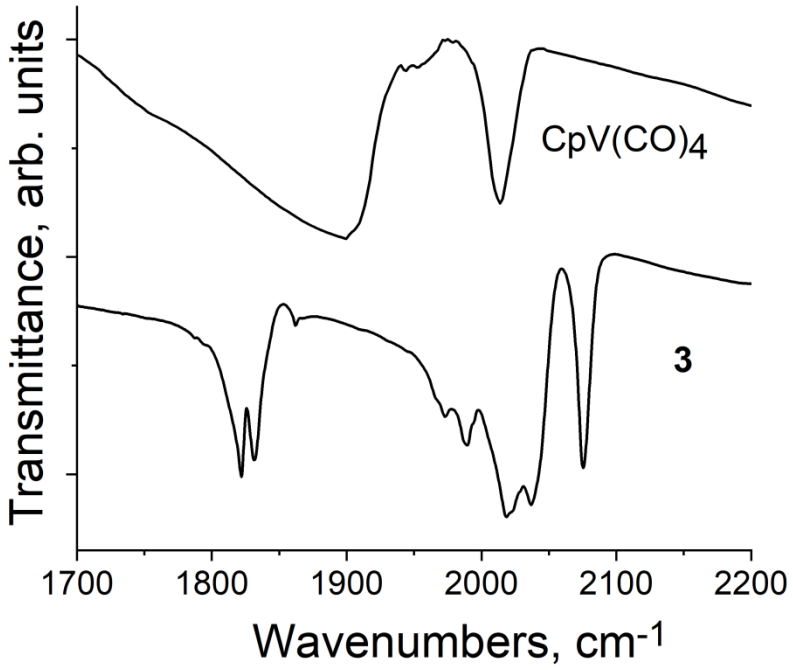

Figure S2. IR spectra of starting transition metal complex and salt **3** in 1700 – 2200 cm^{-1} range in KBr pellets prepared in anaerobic conditions

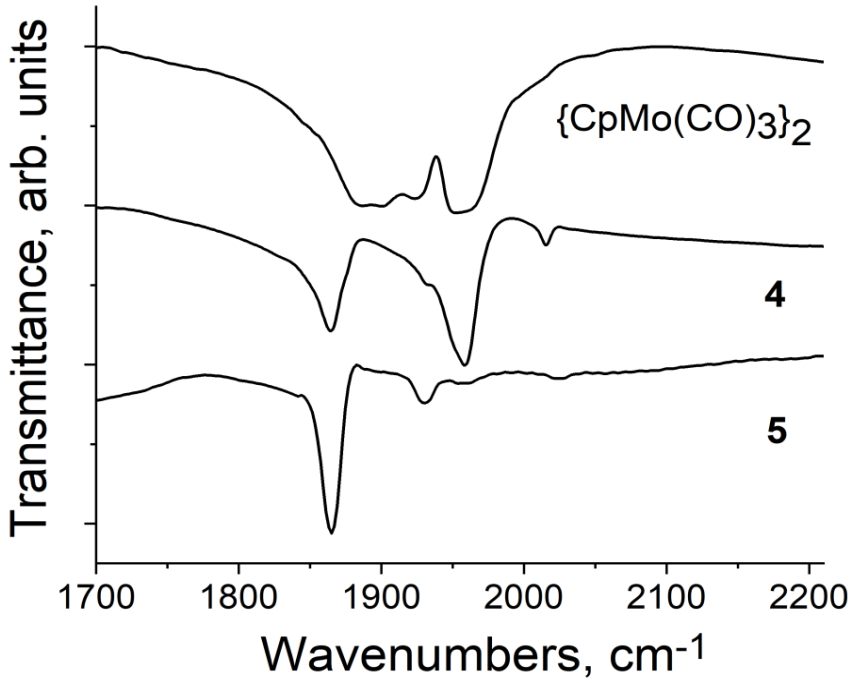

Figure S3. IR spectra of starting transition metal complex and salts **4** and **5** in 1700 – 2200 cm^{-1} range in KBr pellets prepared in anaerobic conditions.

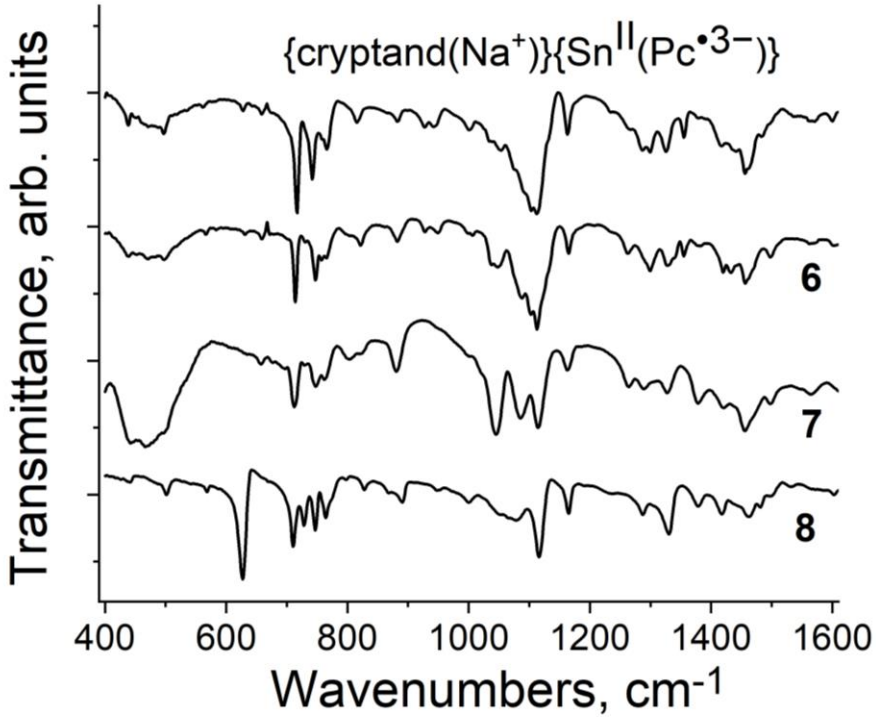

Figure S4. IR spectra of radical anion salt {cryptand(Na^+)} $[Sn^{II}(Pc^{\bullet 3-})]^{\bullet -}\cdot C_6H_4Cl_2$ and salts **6 - 8** in KBr pellets prepared in anaerobic condition.

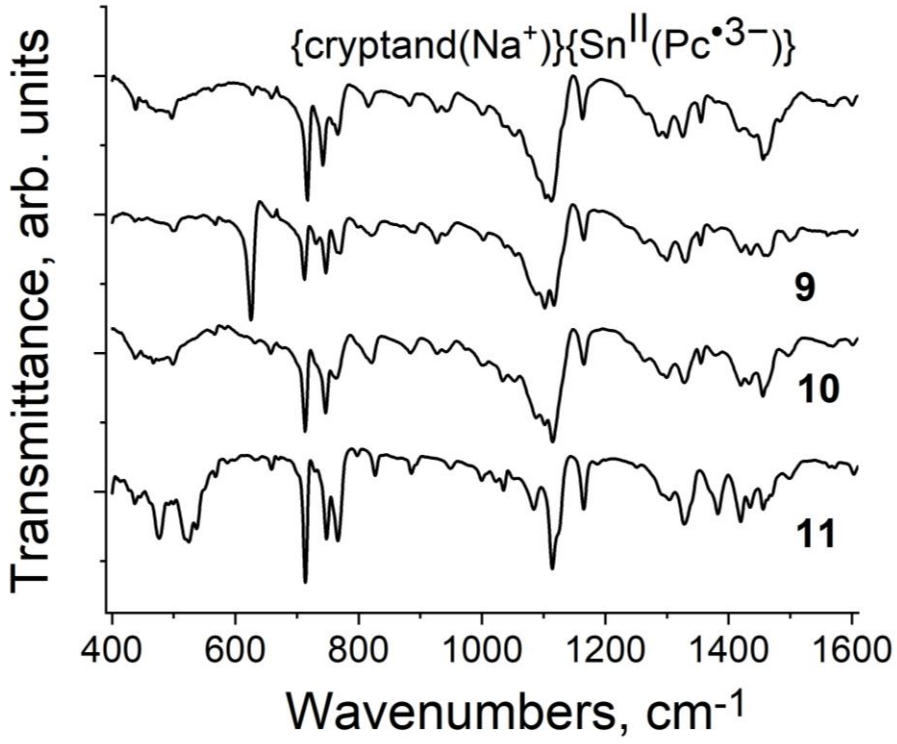

Figure S5. IR spectra of radical anion salt {cryptand(Na^+)} $[Sn^{II}(Pc^{\bullet 3-})]^{\bullet -}\cdot C_6H_4Cl_2$ and salts **9 - 11** in KBr pellets prepared in anaerobic condition.

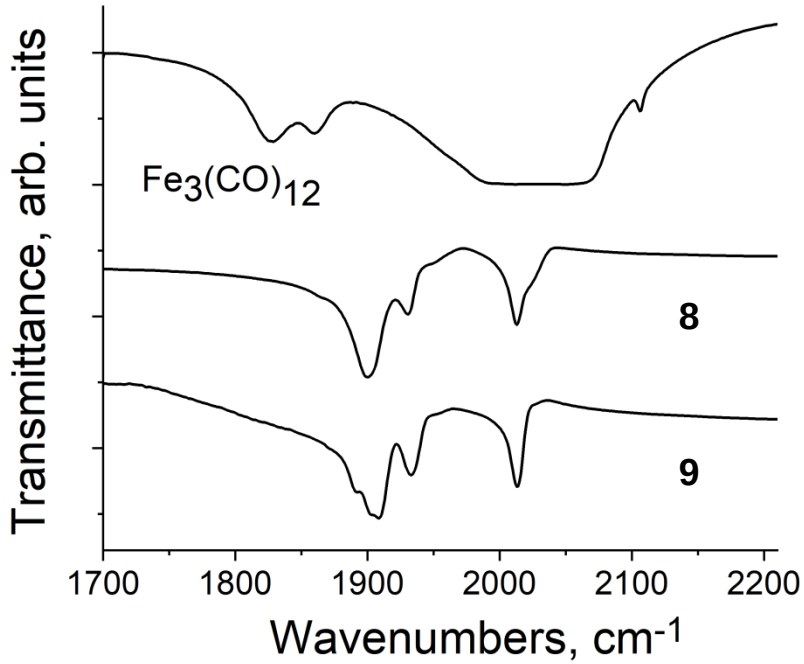

Figure S6. IR spectra of starting transition metal complex $Fe_3(CO)_{12}$ and compounds **8** and **9** in 1700 – 2210 cm^{-1} range in KBr pellets prepared in anaerobic conditions.

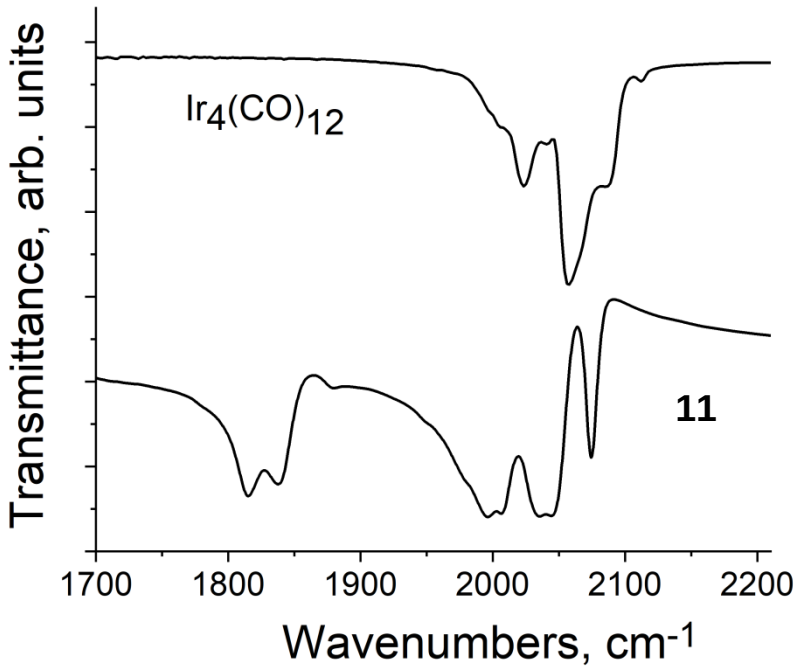

Figure S7. IR spectra of starting transition metal complex and salt **11** in 1700 – 2210 cm^{-1} range in KBr pellets prepared in anaerobic conditions.

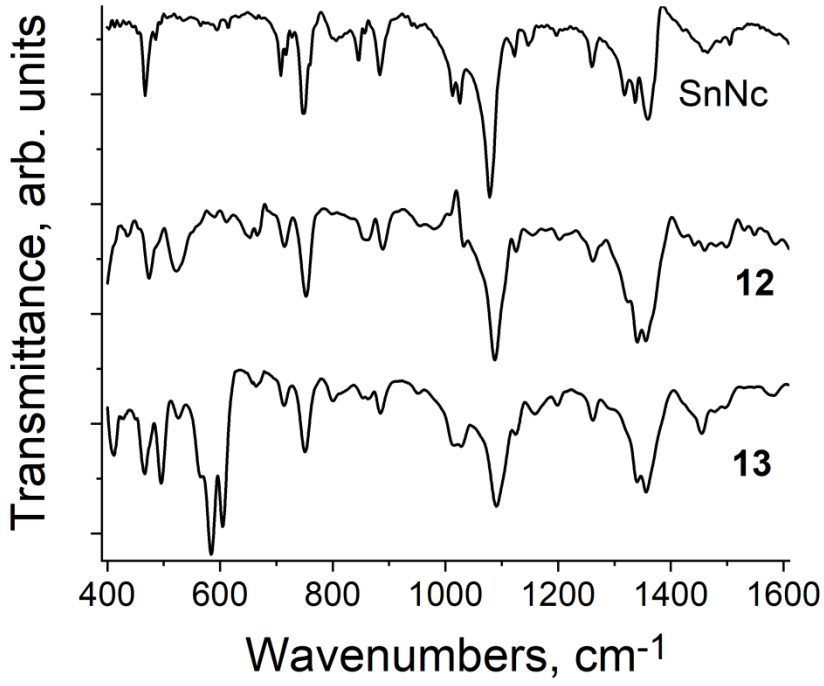

Figure S8. IR spectra of pristine neutral SnNc and compounds **12** and **13** in KBr pellets prepared in anaerobic condition.

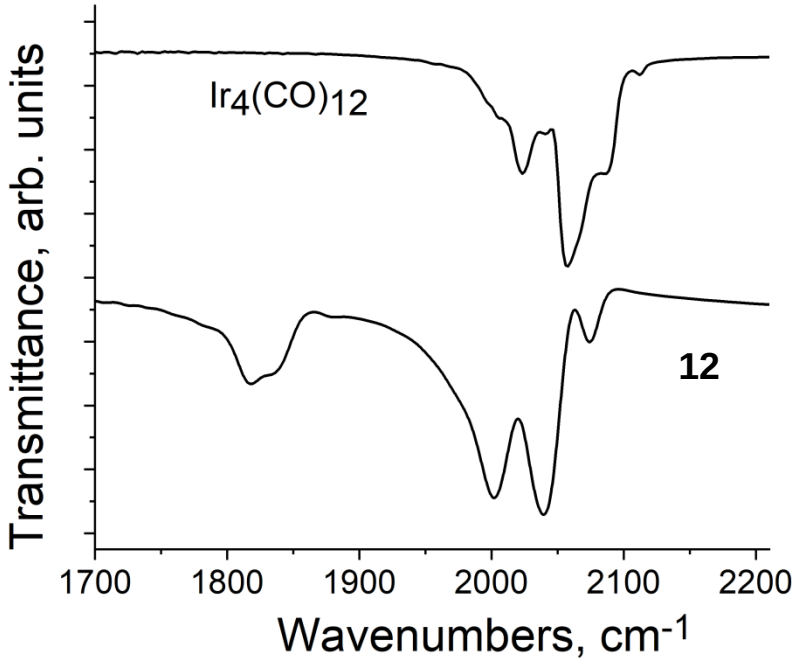

Figure S9. IR spectra of starting transition metal complex $Ir_4©_{12}$ and compound **12** in 1700 – 2200 cm^{-1} range in KBr pellets prepared in anaerobic conditions.

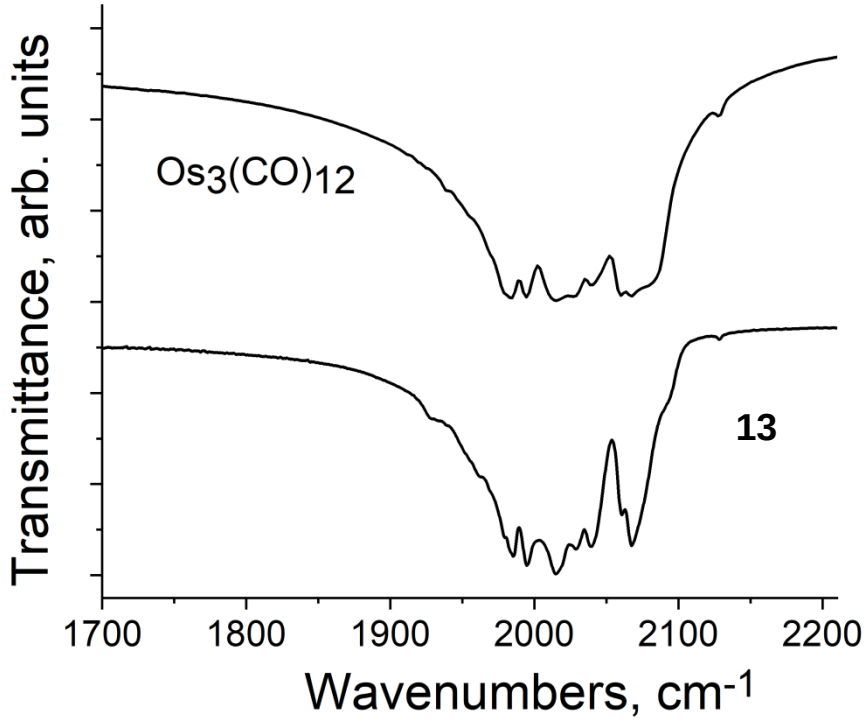

Figure S10. IR spectra of starting transition metal carbonyl $Os_3(CO)_{12}$ and compound **13** in 1700 – 2210 cm^{-1} range in KBr pellets prepared in anaerobic conditions.

Spectra in the UV-visible-NIR range.

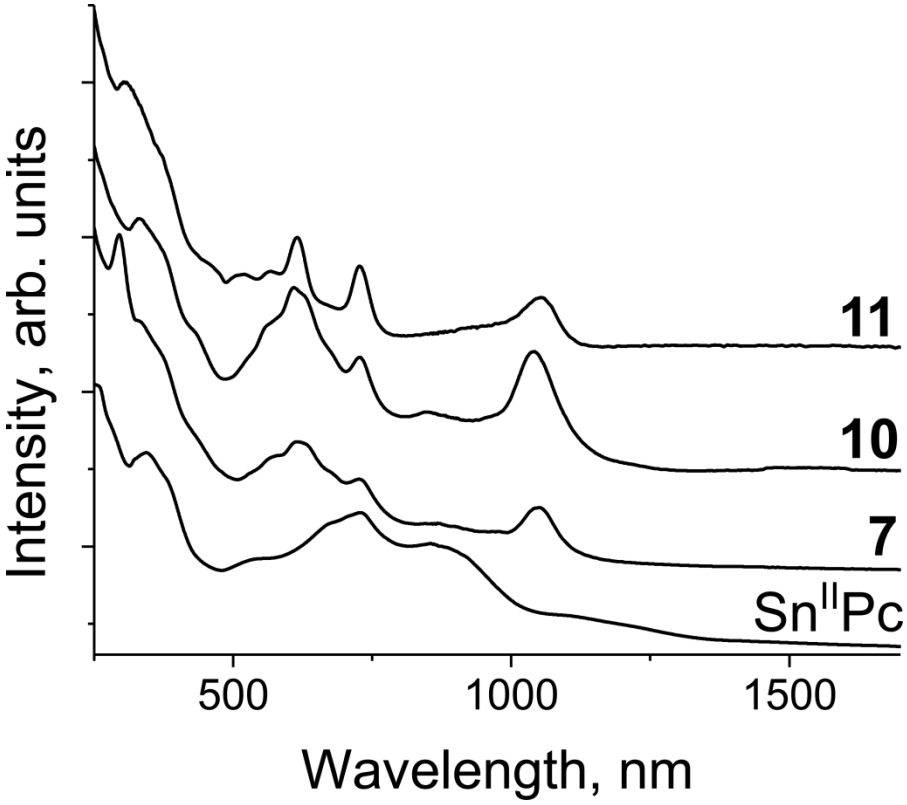

Fig. S11a. UV-visible-NIR spectra of coordination complexes of transition metals with the $\{Sn^{II}(Pc^{\bullet 3-})\}^{-}$ radical anions in **8**, **11-12** measured in KBr pellets prepared in anaerobic conditions.

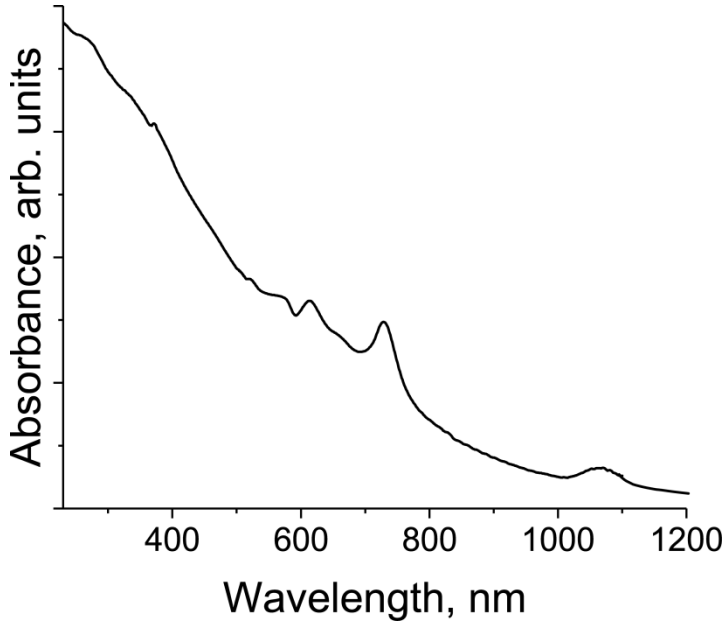

Fig. S11b. UV-visible-NIR spectra of coordination complex **5** measured in KBr pellets prepared in anaerobic conditions.

Crystal structures.

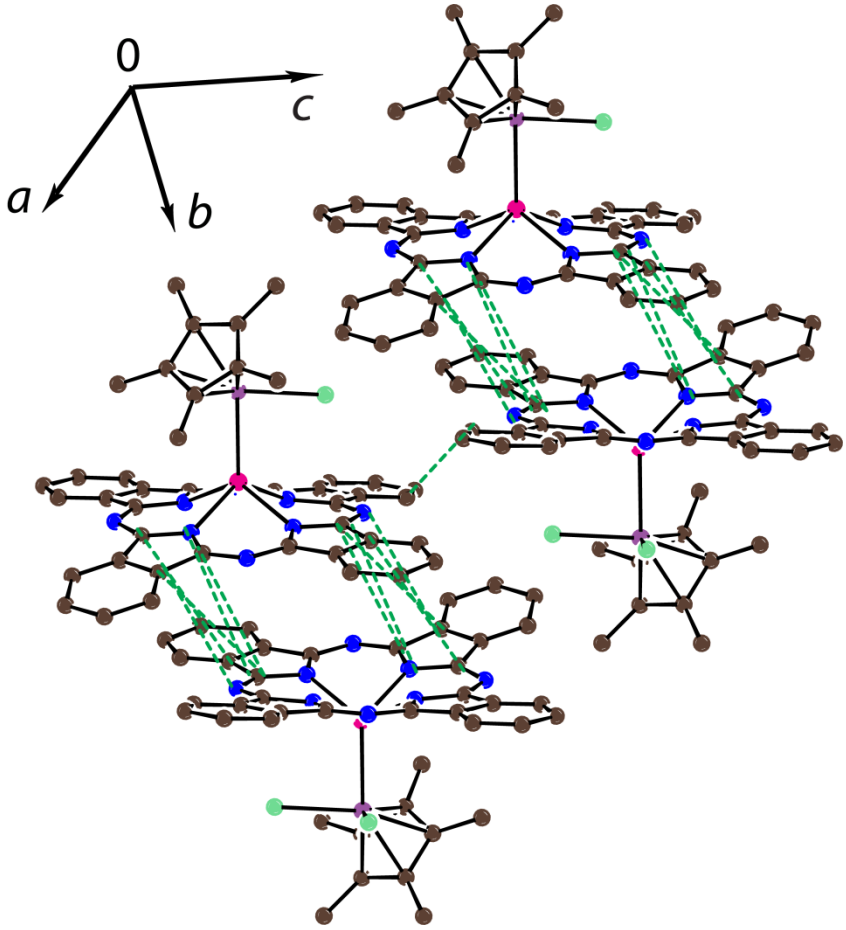

Figure S12a. Crystal structure of [Cp*$IrCl_2$·Sn^{II}(Pc^{2-})] (**1**). Ortep drawing with equivalent isotropic atomic displacement parameters is shown.

.

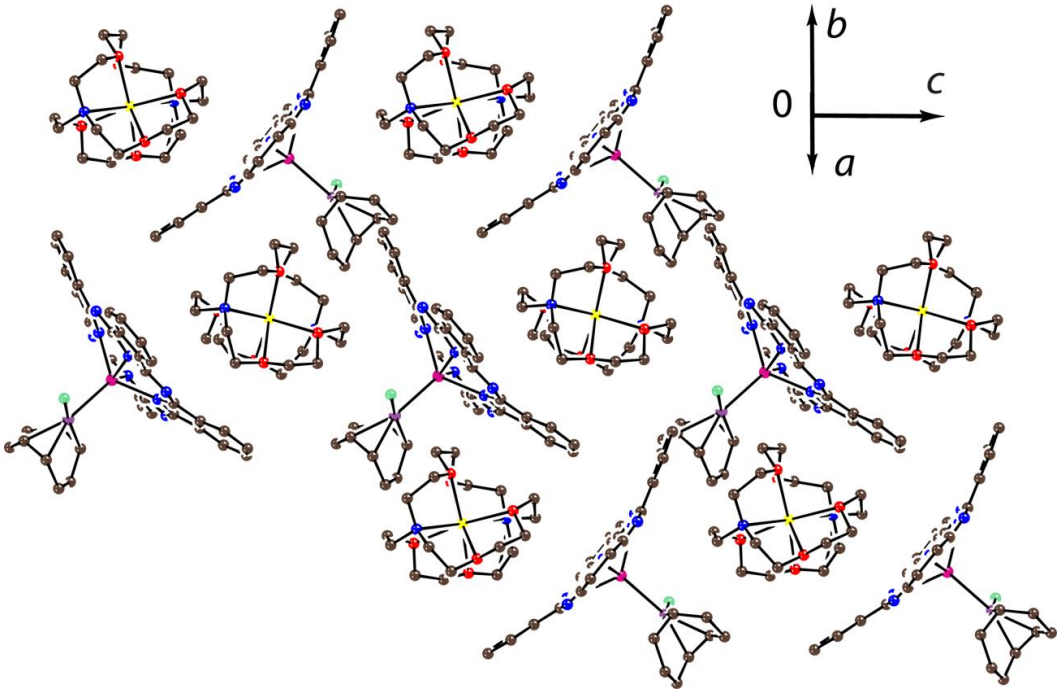

Figure S12b. Crystal structure of {Cryptand(Na^+))[(COD)IrCl·$Sn^{II}(Pc^{\bullet 3-})$]$^-$·2$C_6H_4Cl_2$ (**6**). Solvent $C_6H_4Cl_2$ molecules are not depicted. Ortep drawing with equivalent isotropic atomic displacement parameters is shown.

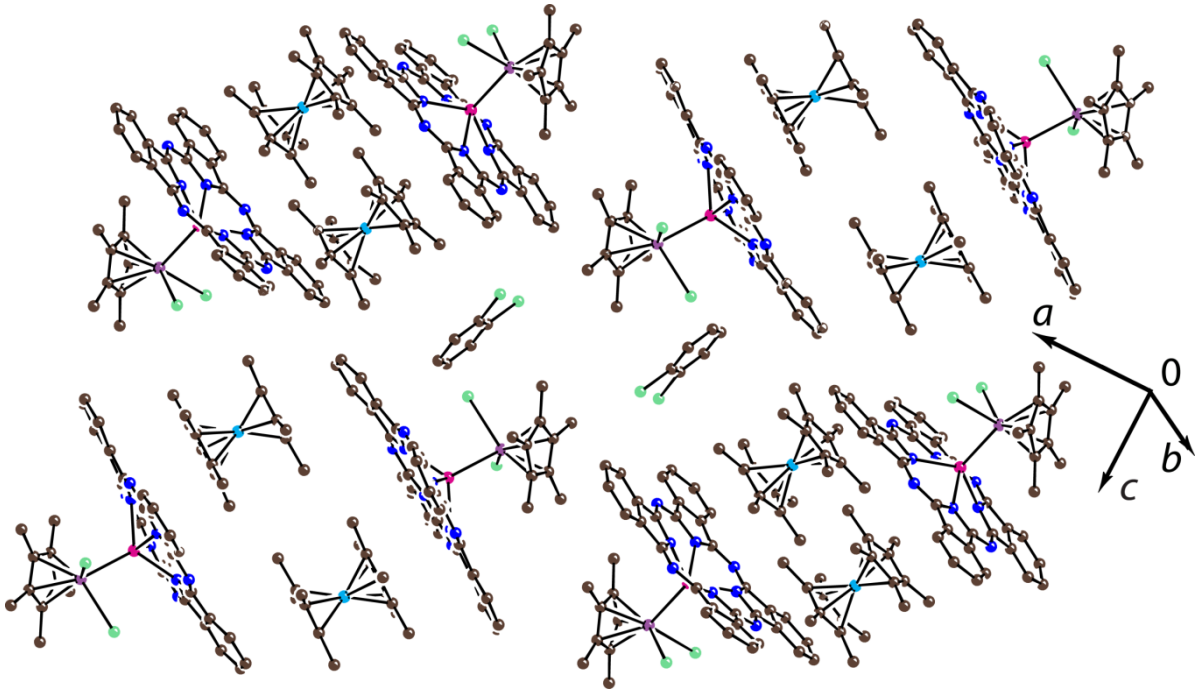

Figure S13. Crystal structure of $\{Cp^*_2Co^+)[Cp^*IrI_2{\cdot}Sn^{II}(Pc^{\bullet 3-})]^-{\cdot}2C_6H_4Cl_2$ (**7**). Ortep drawing with equivalent isotropic atomic displacement parameters is shown.

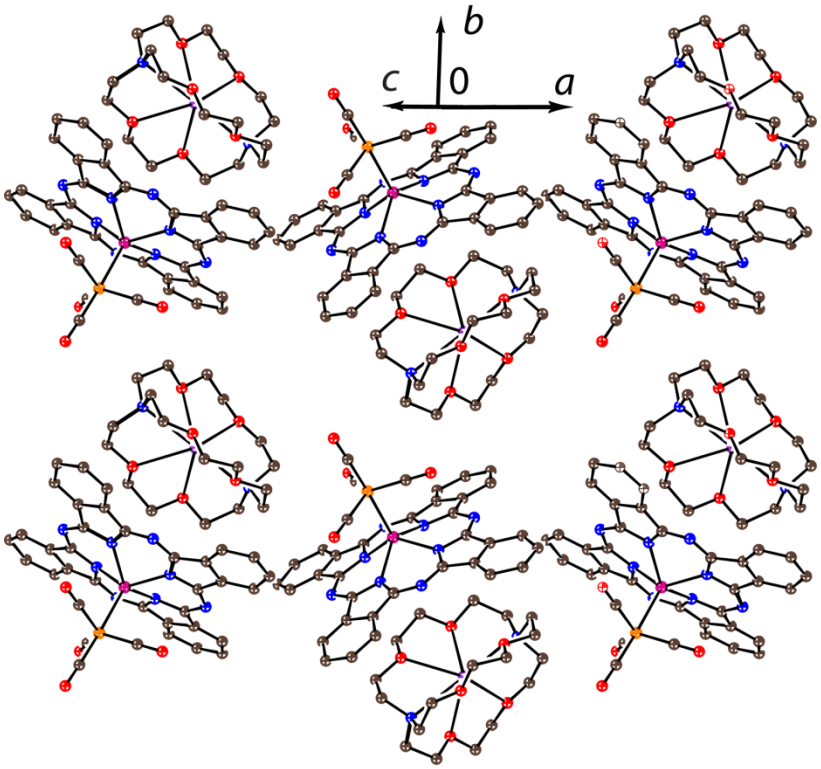

Figure S14. Crystal structure of {Cryptand(Na^+))[$Fe(CO)_4$·$Sn^{II}(Pc^{\bullet 3-})$]·$2C_6H_4Cl_2$ (**9**). Solvent $C_6H_4Cl_2$ molecules are not depicted. Ortep drawing with equivalent isotropic atomic displacement parameters is shown.

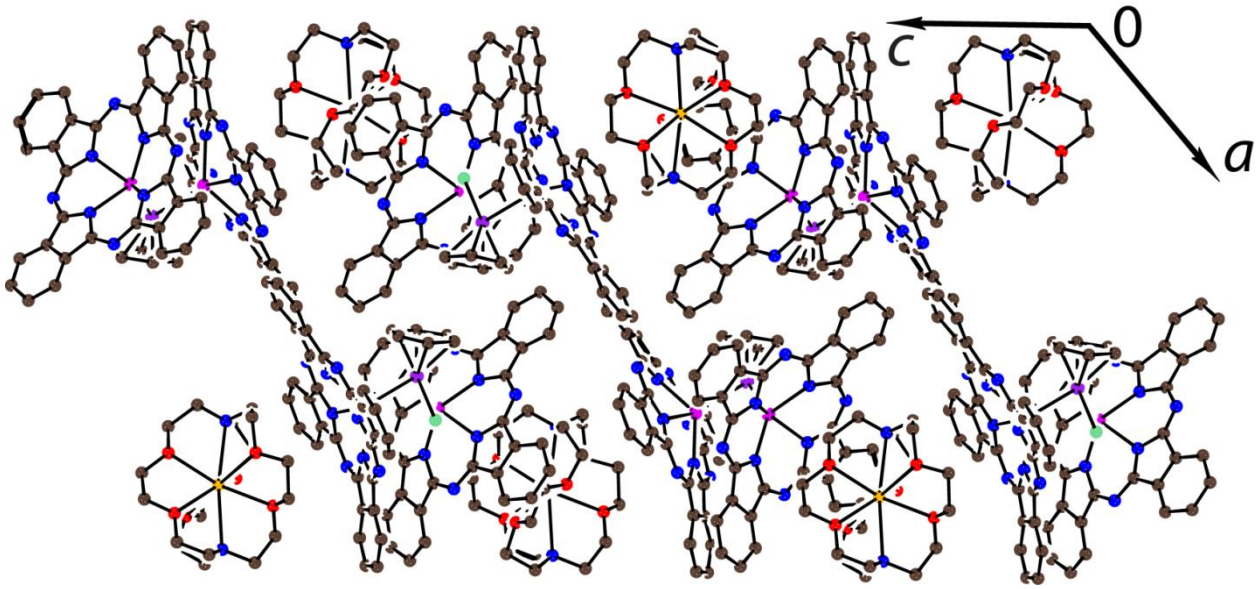

Figure S15. Crystal structure of {Cryptand(Na^{+})}[(C_6H_6)$RuCl_2$·{$Sn^{II}(Pc^{\bullet 3-})$}$_2$]·$C_6H_4Cl_2$ (**10**). Solvent $C_6H_4Cl_2$ molecules are not depicted. Ortep drawing with equivalent isotropic atomic displacement parameters is shown.

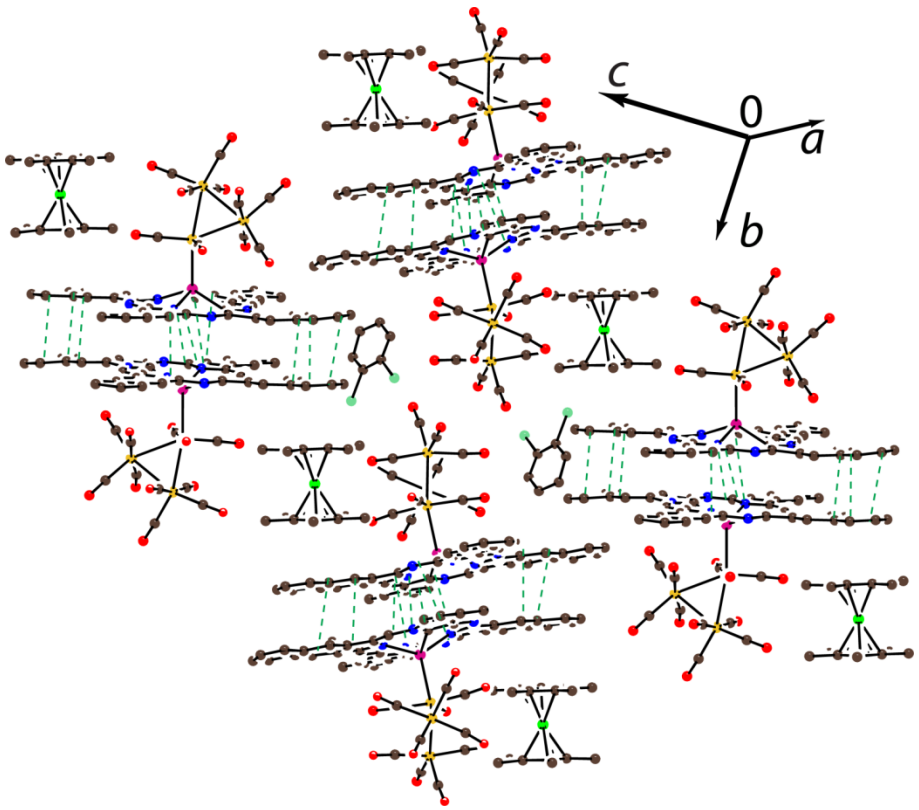

Figure S16. Crystal structure of $\{Cp^*_2Cr^+)[Os_3(CO)_{11}\cdot Sn^{II}(Nc^{\bullet 3-})]^-2C_6H_4Cl_2$ (**13**). Ortep drawing with equivalent isotropic atomic displacement parameters is shown. Van der Waals C,N…C,N contacts are shown by green dashed lines.

Magnetic data for 6

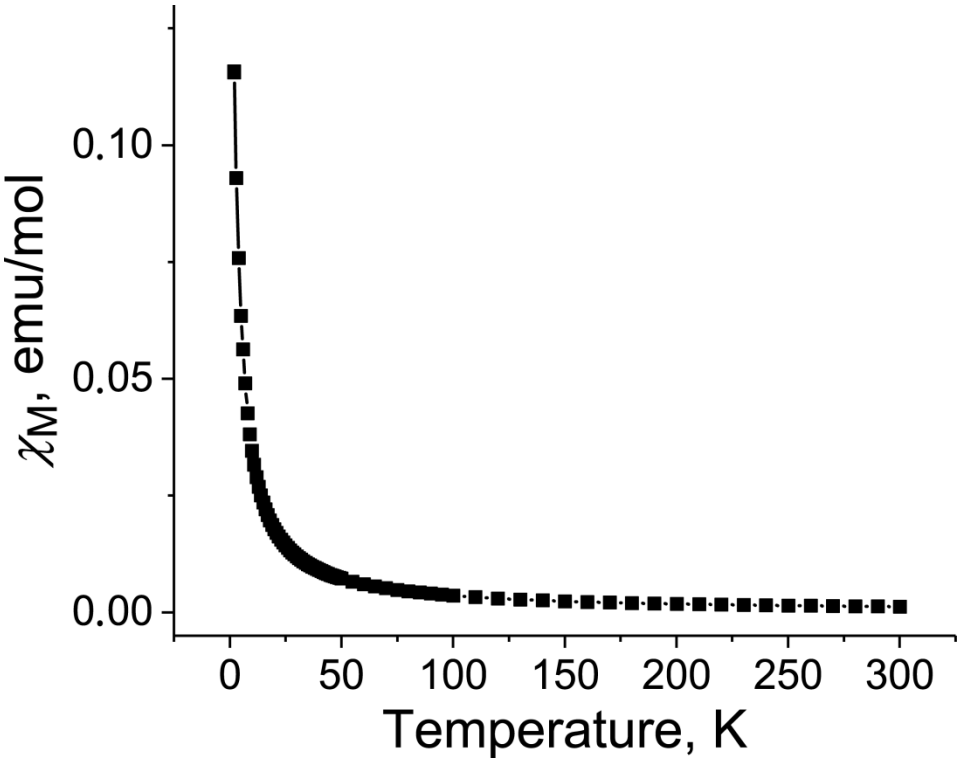

Figure S17. Temperature dependence of molar magnetic susceptibility of polycrystalline **6**.

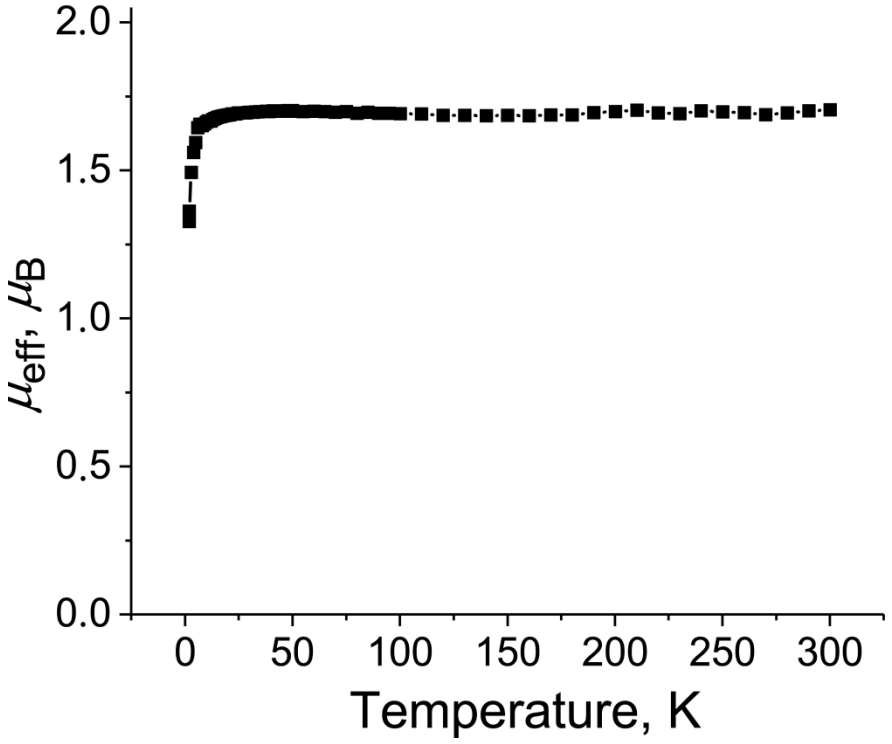

Figure S18. Temperature dependence of effective magnetic moment of polycrystalline **6**

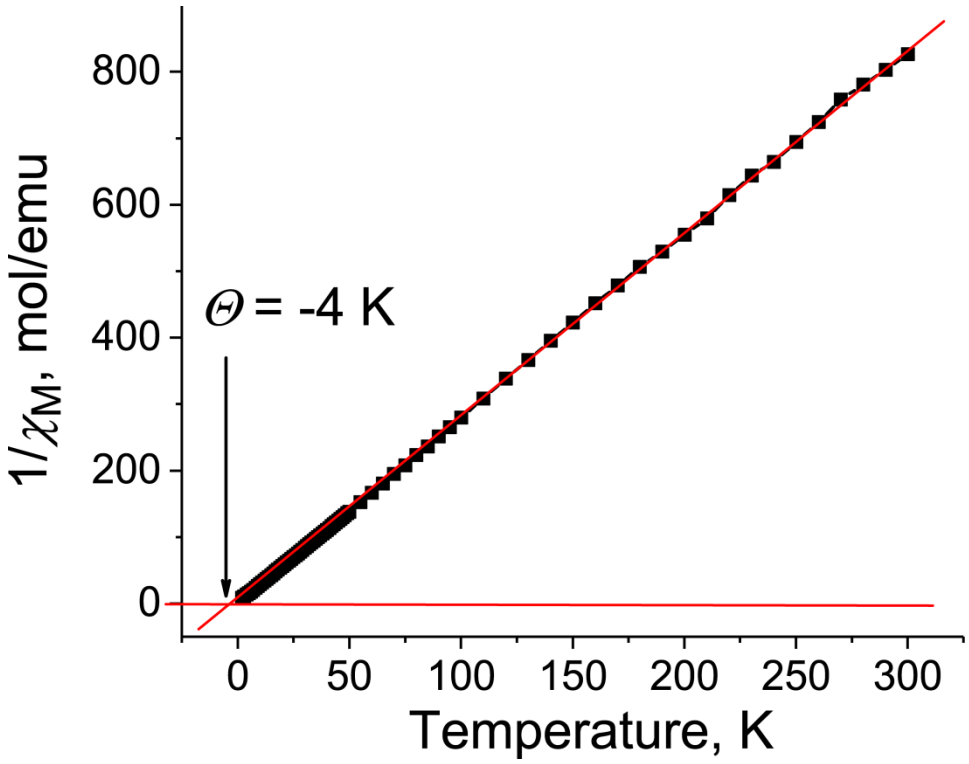

Figure S19. Temperature dependence of reciprocal molar magnetic susceptibility of polycrystalline **6**.

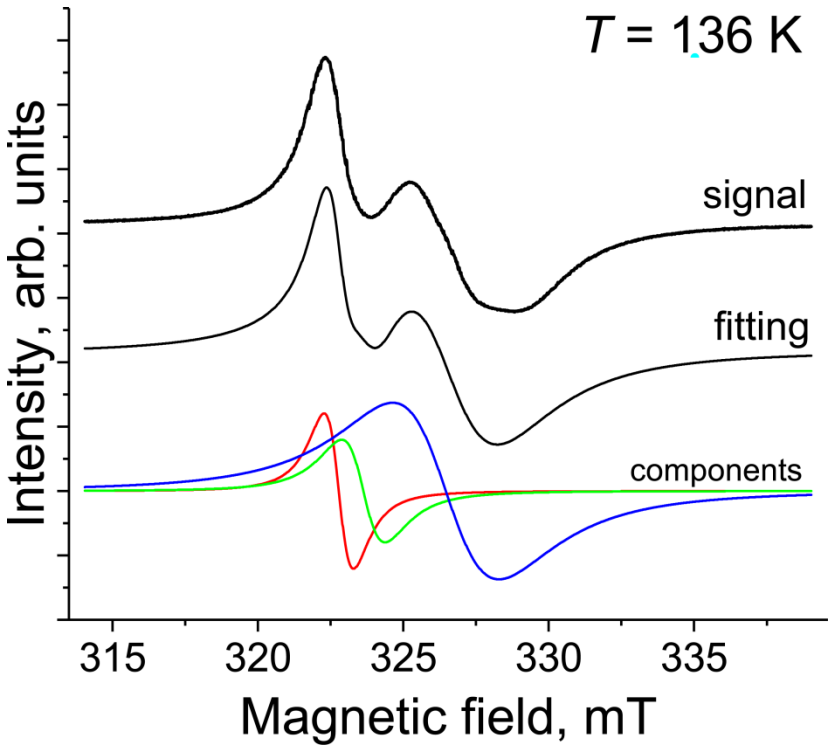

Figure S20. EPR spectrum of polycrystalline **6** at 136 K.

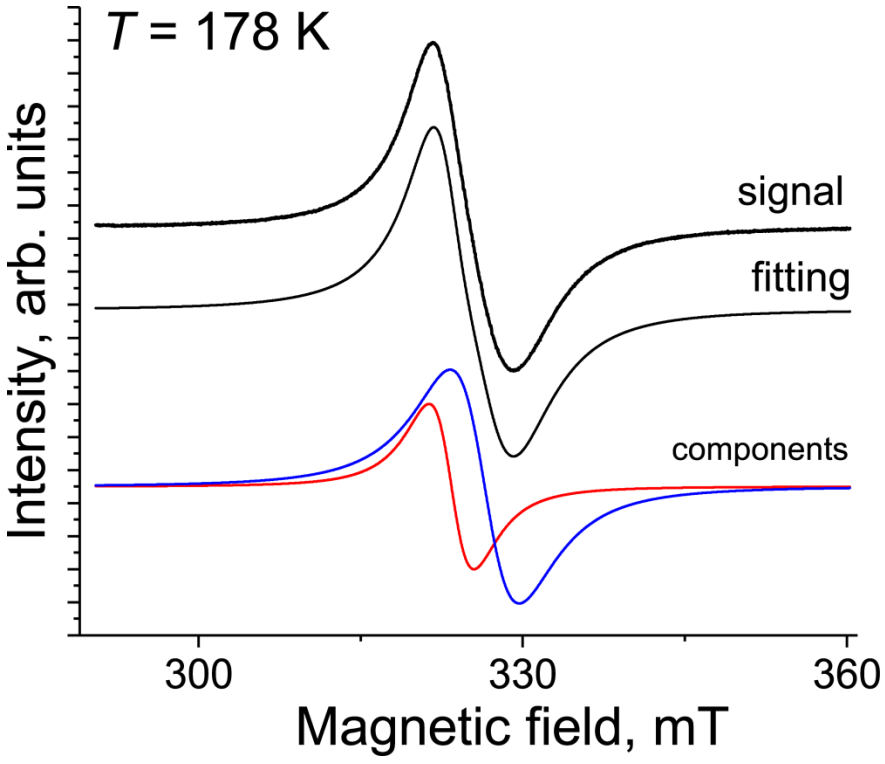

Figure S21. EPR spectrum of polycrystalline **6** at 178 K.

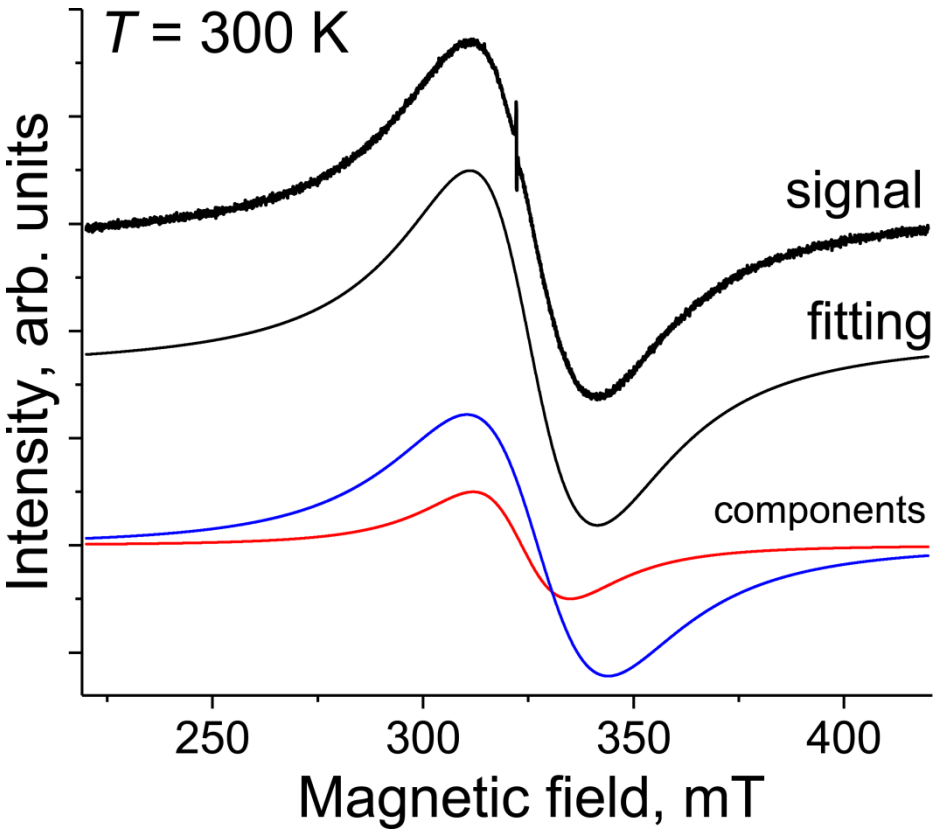

Figure S22. EPR spectrum of polycrystalline **6** at 300 K.

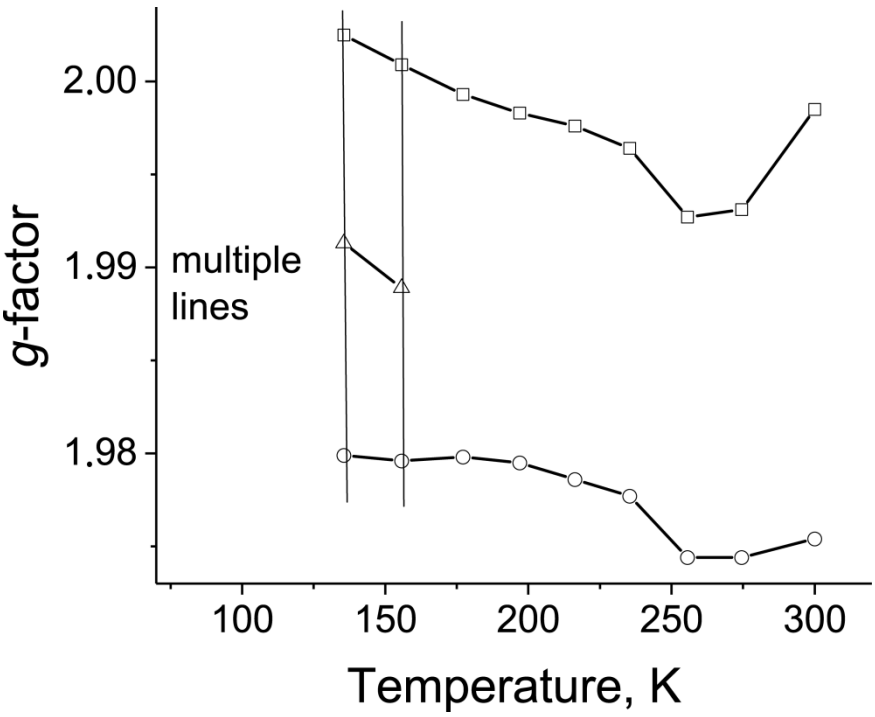

Figure S23. Temperature dependence of *g*-factors of the components of EPR signal from polycrystalline **6**.

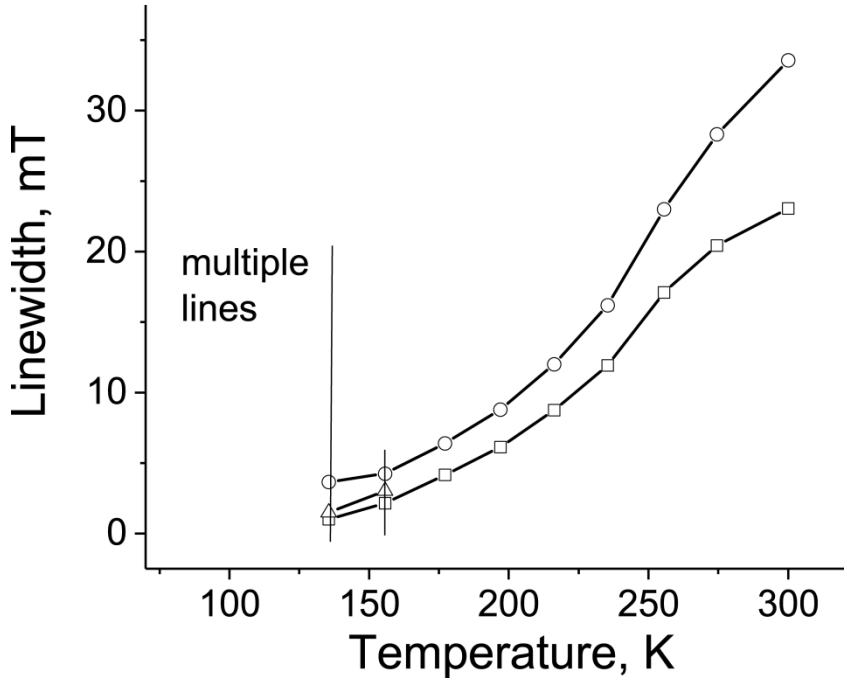

Figure S24. Temperature dependence of the linewidth of the components of EPR signal from polycrystalline **6**.

Magnetic data for 11.

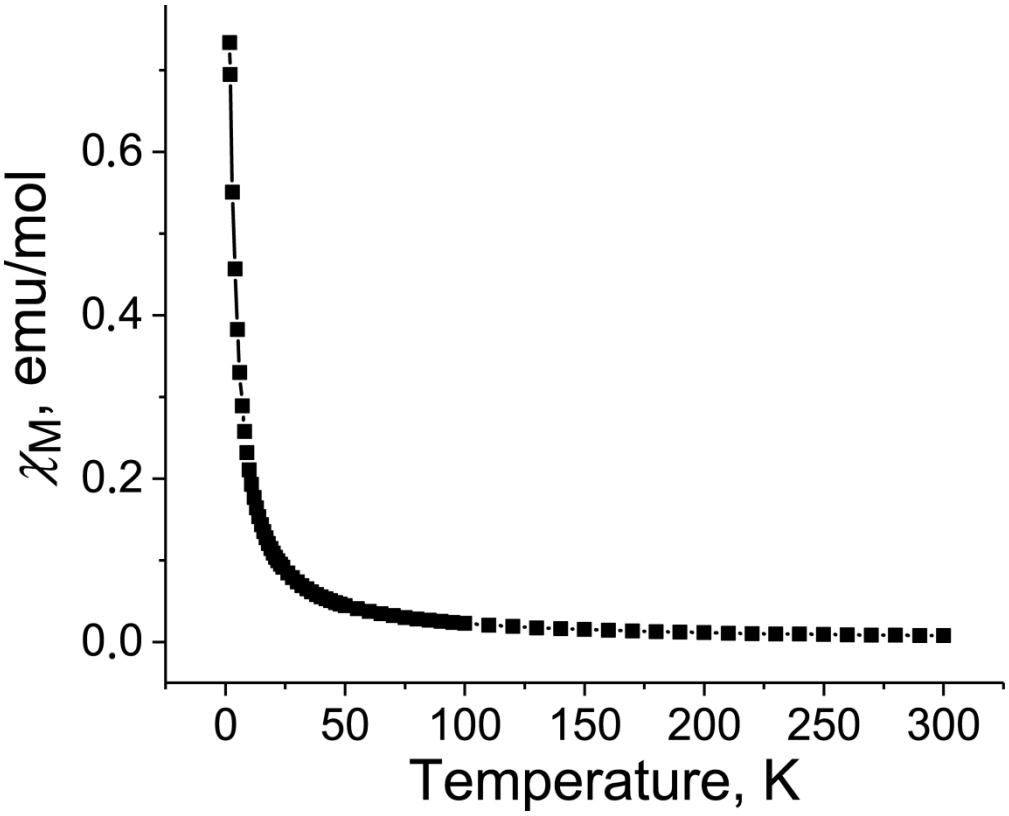

Figure S25. Temperature dependence of molar magnetic susceptibility of polycrystalline **11.**

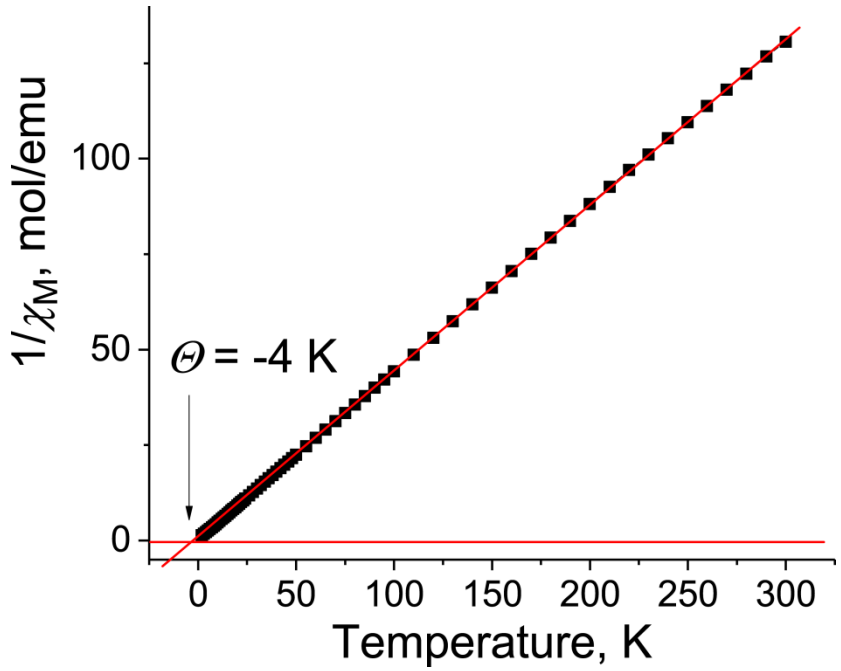

Figure S26. Temperature dependence of reciprocal molar magnetic susceptibility of polycrystalline **11.**

Magnetic data for 12.

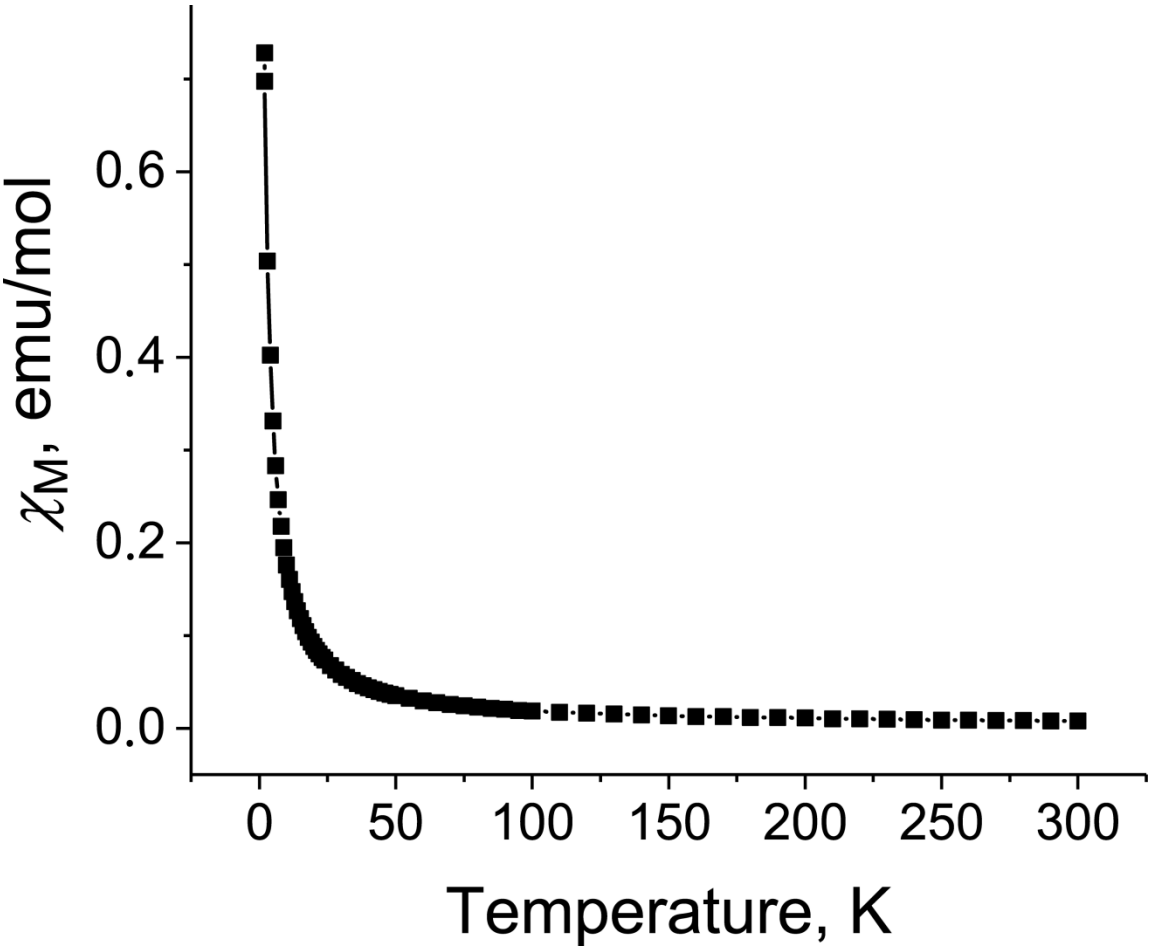

Figure S27. Temperature dependence of molar magnetic susceptibility of polycrystalline **12.**